Abundances and physical parameters for stars in the open clusters NGC 5822 and IC 4756. [*]

G. Pace[1], J. Danziger[2,3], G. Carraro[4], J. Melendez[1], P. François[5], F. Matteucci[2,3], and N. C. Santos[1]

[1] Centro de Astrofisica, Universidade do Porto, Rua das Estrelas, 4150–762 Porto, Portugal

[2] INAF, Osservatorio Astronomico di Trieste, via G.B. Tiepolo 11, 34131 Trieste, Italy

[3] Department of Astronomy, University of Trieste, via G.B. Tiepolo 11, 34131 Trieste, Italy

[4] European Southern Observatory, Casilla 19001, Santiago, Chile

[5] Observatoire de Paris, 64 Avenue de l'Observatoire, 75014 Paris, France

ABSTRACT

Context. Classical chemical analyses may be affected by systematic errors that would cause observed abundance differences between dwarfs and giants. For some elements, however, the abundance difference could be real.
Aims. We address the issue by observing 2 solar–type dwarfs in NGC 5822 and 3 in IC 4756, and comparing their composition with that of 3 giants in either of the aforementioned clusters. We determine iron abundance and stellar parameters of the dwarf stars, and the abundances of calcium, sodium, nickel, titanium, aluminium, chromium, silicon, and oxygen for both the giants and dwarfs. For the dwarfs, we also estimate the rotation velocities, and and lithium abundances. We improve the cluster parameter estimates (distance, age, and reddening) by comparing existing photometry with new isochrones.
Methods. We acquired UVES high–resolution, of high signal–to–noise ratio (S/N) spectra. The width of the cross correlation profiles was used to measure rotation velocities. For abundance determinations, the standard equivalent width analysis was performed differentially with respect to the Sun. For lithium and oxygen, we derived abundances by comparing synthetic spectra with observed line features.
Results. We find an iron abundance for dwarf stars equal to solar to within the margins of error for IC 4756, and slightly above for NGC 5822 ([Fe/H]= 0.01 and 0.05 dex respectively). The 3 stars in NGC 4756 have lithium abundances between Log N(Li)≈ 2.6 and 2.8 dex, the two stars in NGC 5822 have Log N(Li)≈ 2.8 and 2.5, respectively.
Conclusions. For sodium, silicon, and titanium, we show that abundances of giants are significantly higher than those of the dwarfs of the same cluster (about 0.15, 0.15, and 0.35 dex). Other elements may also undergo enhancement, but all within 0.1 dex. Indications of much stronger enhancements can be found using literature data. But artifacts of the analysis may be partly responsible for this.

Key words. Open clusters: individual: – stars: abundances

1. Introduction

Several projects to determine open cluster chemical abundances and parameters are being carried out, such as that of BOCCE (Bragaglia & Tosi 2006), in which chemical abundances of stars in the red clump of open clusters are measured, red clump stars being giants that are burning helium in their core. BOCCE, with many singular or coordinated studies of stars of different spectral type and luminosity class, has significantly enhanced the database

that can be employed to determine the Galactic abundance gradient (e.g., Carraro et al. 2007; Magrini et al. 2009; D'Orazi & Randich 2009; Paulson et al. 2003). These studies aim mainly to investigate the evolution with time of several phenomena occurring in stars, such as the depletion of light elements and chromospheric activity, and global properties of the Galactic disk, such as the metallicity gradient and the age–metallicity relationship (e.g., Carraro et al. 1998; Friel et al. 2002; Magrini et al. 2009).

Targeting open clusters is justifiable for several reasons: they are single stellar populations, i.e., ensembles of stars with a common age, chemical composition, and distance; they are distributed across the entire Galactic disk; and they span a wide range of ages. Only very young clusters tend to cluster close to the spiral arms, where they recently formed (Dias & Lépine 2005). High resolution spectra allow us to measure the abundance of light elements and in

---

particular lithium, which is an invaluable probe of the mixing mechanisms in stellar envelopes. Smiljanic et al. (2009) obtained very interesting results by studying lithium and beryllium in several IC 4651 members at different evolutionary stages. Both elements are fragile but are destroyed at different temperatures, i.e., in different layers, and therefore probe the stellar interior at different depths.

In addition to the depletion of light elements, we investigate whether the chemical composition changes during evolutionary transitions in the stellar lifetime, for which open cluster are suited particularly well. Sodium and aluminium have been found by several authors to be overabundant in giants belonging to several open clusters, for instance IC 4756, NGC 6939 and NGC 714 (Jacobson et al. 2007), NGC 6475 (Villanova et al. 2009), Collinder 261 (Friel et al. 2003), Berkeley 17 (Friel et al. 2005), and Saurer 1 and Berkeley 29 (Carraro et al. 2004). For some other clusters, only sodium overabundances were inferred in giants: IC 4651 (Pasquini et al. 2004), NGC 7789 and M 67 (Tautvaišiene et al. 2000; Tautvaišienė et al. 2005; Randich et al. 2006), and NGC 1817 and NGC 2141 (Jacobson et al. 2009). In some of these studies, a direct comparison between evolved and unevolved stars was possible, and sodium and aluminium abundances in evolved stars were found to be higher than in dwarfs. In other studies, the overabundances were detected just as an abundance ratio [Na–Al/Fe] greater than 0.1 dex in giants or clump stars. Randich et al. (2006) argue that sodium enhancement in M 67 should be ascribed to non–LTE effects affecting sodium lines in giants more than dwarfs, as discussed in Mashonkina et al. (2000). The extreme sensitivity of sodium to non–LTE effects was also noted by Sestito et al. (2007). Incorrect gf values may also play a major role for giant stars, since, unlike dwarf stars, their differential analysis with respect to the Sun may not overcome this problem. But in some of the clusters mentioned above, the effect may be in part real, since the amount of enhancement found varies significantly from cluster to cluster, even when the same kind of analysis is performed. In this case, aluminium and sodium enhancements may be caused by internal processes.

Whether real or an artifact of the analysis, abundance differences between evolved and unevolved stars have important implications because they mean that spurious differences may be found between stellar samples, if care has not been taken in comparing only dwarfs with dwarfs, or giants with giants.

In the present study, we analyse 5 solar–type stars in the open clusters IC 4756 and NGC 5822, and we compare our results with those for giants of the same clusters. These clusters were studied with other open clusters by Santos et al. (2009). In this paper, iron abundances are analysed and we determine the chemical abundances of several other elements.

The paper is organised in the following way. In Sect. 2, we describe the sample and the observations. In Sect. 3, we report the chemical abundance measurements with special emphasis on oxygen and lithium. An estimate of the projected rotation velocity of the sample stars is given in Sect. 4. In Sect. 5, we discuss the difference between giants and dwarfs, using both our chemical abundance measurements and previously published results. In Sect. 6, we evaluate the cluster parameters by fitting isochrones to the colour–magnitude diagrams. Finally, we summarise the content of the paper in Sect. 7.

2. Observations and sample

The data analysed consist of UVES spectra of 5 dwarf and 6 giants members of NGC 5822 and IC 4756.

The observations of the dwarf stars were designed to determine the evolution in the chromospheric activity of solar–type stars, and carried out in the ESO observing run 073.D-0655. The clusters, IC 4756 and NGC 5822, were chosen mainly because of their intermediate age of about 1 Gyr, NGC 5822 being slightly younger than IC 4756. Target stars were selected from all solar–type, single members. Photometric data used in this selection, including target names, were taken from Herzog et al. (1975) for IC 4756 and from Twarog et al. (1993) for NGC 5822. For the same clusters, UVES spectra of 6 giants were made available to ourselves. A detailed description of the giant spectra is given in Santos et al. (2009) and is not repeated here.

Between 2 and 7 spectra were taken for each dwarf of the initial sample using UVES on the VLT at a resolution of about R= 100 000 in the red arm, which covers the range from 4 800 to 6 800 Å. Radial velocity measurements were used to strengthen single–member selection. They were obtained by cross–correlating stellar spectra with that of the Sun using the IRAF command $f$xcor.

We detected the following double stars in IC 4756: HER 40, HER 150, HER 183, HER 189, and HER 294. The stars HER 150, HER 189, and HER 294 are double–lined and the other binaries were detected because of a radial velocity variation larger than 1 km·sec^{-1}. We were left with only 3 single members for this cluster, namely HER 97, HER 165, and HER 240, which each had 2 observations on two different nights: their radial velocity differences of, respectively, 0.06, 0.20 and 0.40 km·sec^{-1} are attributable to measurement errors. Their radial velocities are -24.9, -25.7, -24.9 km·sec^{-1}, which confirm their membership when assuming the mean cluster radial velocity of -25.2 km·sec^{-1} (Jacobson et al. 2007; Mermilliod et al. 2008). The cluster is affected by variable extinction (Schmidt 1978); therefore the use of photometric information to select the targets (Herzog et al. 1975) may not have prevented a large proportion of double stars from being included in the original sample.

After adding the spectra, the resulting S/N per pixel for these stars was about 50 in the blue arm and 100 in the red arm. The HER 97 spectra are of slightly poorer quality than those of the other two stars, which probably explains the larger difference between the 2 radial velocity measurements.

In NGC 5822, we observed TATM 11014 seven times, and TATM 11003 four times in a total of 6 different nights. Their radial velocities for the individual observations have a standard deviation of about 0.5 km·sec^{-1} for both stars, which we attribute to the measurement errors. The S/N of the single spectra can be, in fact, as low as 20.

The radial velocity of TATM 11003 is -29.1 km·sec^{-1}, and that of TATM 11014 is -27.9 km·sec^{-1}. The mean radial velocities of the 20 confirmed members of NGC 5822 studied by Mermilliod & Mayor (1990) have a distribution whose mean value is -29.3 km·sec^{-1}, with a standard deviation of about 0.8 km·sec^{-1}, thus confirming the membership of our target stars. After coadding all the spectra

of each star, we achieved a S/N of 50 for the blue arm of TATM 11014 and slightly more than 100 for the red arm for the same star, and about 60 and 30 for the red and blue arm of TATM 11003, respectively. We used some of the spectra used in Pace & Pasquini (2004), including the solar spectrum from the UVES archive, to calibrate the rotation velocity (Sect. 4) and measure lithium abundances (Sect. 3.2).

3. Chemical abundances

To measure the stellar parameters of dwarf stars, i.e., temperature, gravity, microturbulent velocity, and the abundances of iron, calcium, sodium, nickel, titanium, aluminium, chromium, and silicon, we employed the same procedure and error analysis used in Pace et al. (2008), to which we refer the reader for a detailed description. Suffice it to say that we performed a standard EW analysis, i.e., we measured EWs and inferred abundances for each individual line (in the case of iron in two ionization states) by means of OSMARCS LTE models (Edvardsson et al. 1993), differentially line by line with respect to the Sun, and that the adopted atmospheric parameters were chosen among a grid of trial values. The only difference between the present analysis of dwarf stars and that of Pace et al. (2008), is that the temperature estimates about which the grids of parameters were constructed, were obtained from the B-V colours published in Herzog et al. (1975) and Twarog et al. (1993) through the calibrations in Soderblom et al. (1993) and Casagrande et al. (2006). To deredden the colours, we used the E(B-V) values computed in Sect. 6.

As for giant stars, stellar parameters and iron abundances were determined in Santos et al. (2009) using the line list of either Sousa et al. (2008, S08) or that of Hekker & Meléndez (2007, HM). Effective temperature and gravity measurements in the two sets agree to within the margins of error, while the iron abundances obtained using HM are between 1 and 2 σ higher. We determined the stellar parameters for giants using the same procedure and line list as for dwarfs, and we show in Table 1 a comparison between our results, labelled "R06", and those of Santos et al. (2009), labelled either "S08" or "HM" according to the line list adopted. Our measurements match the results obtained using HM, and we used them to proceed, in the same way as for dwarfs, with the measurement of calcium, sodium, nickel, titanium, aluminium, chromium, silicon and oxygen abundances. In Santos et al. (2009), the preliminary results of the dwarf iron abundances presented here were compared to the giant abundances. We do not have new elements to add to that discussion, and we do not repeat it here.

The equivalent width measurements and the relative individual abundances are available at CDS in electronic form (Table 2). Some of them are made automatically with the program ARES Sousa et al. (2007). For a couple of stars, we verified that automatic and interactive measurements are in no poorer agreement than two different sets of measurements performed using the interactive method. The parameters found are indicated in Table 3. In Cols. 2 and 3, we indicate the photometry from Twarog et al. (1993) and Herzog et al. (1975). To deredden B-V, we used the colour excesses obtained in Sect. 6. In the Cols. 4 and 5, we indicate the temperature obtained from the B-V colour by means of the calibrations of Soderblom et al. (1993) and Casagrande et al. (2006), while in Col. 6 we indicate those

obtained in the spectroscopic analysis. The difference between photometric and spectroscopic temperature is extremely large in all dwarfs, spectroscopic temperature being in all cases higher, as was mostly the case in Pace et al. (2008). If we consider photometric temperatures resulting from the calibration in Soderblom et al. (1993), these differences range from about 150 K to 600 K. Expressed in terms of B-V colour, the mismatch amounts to about 0.13 mag for both stars in NGC 5822, and range from 0.05 to 0.17 mag for the stars in IC 4756. The uncertainty in the colour excess computed in Sect. 6 amounts to 0.05 and 0.10 mag for NGC 5822 and IC 4756, respectively. These and the uncertainties in the (B-V)–versus–temperature calibration are unlikely to be the main cause of the discrepancy between spectroscopic and photometric temperatures, since, for instance, the calibration in Casagrande et al. (2006) has a standard deviation of about 50 K. For IC 4756, differential reddening (Schmidt 1978) and the larger photometric errors may account for the mismatch. The spread in the main sequence is of the order of 0.2 mag. In both clusters, there is probably a colour offset in the adopted photometry, possibly caused by an inaccurate transformation from the instrumental to the standard magnitude system. A zeropoint difference of about 0.1 mag or more, which is necessary to explain the mismatch between photometric and spectroscopic temperature, is not rare for photographic photometry when compared to modern CCD studies, and this illustrates the need for new CCD photometry for both clusters. In this study, we therefore rely on the spectroscopic determinations of temperature, which are definitely more trustworthy.

To corroborate the last statement, we show in Fig. 1 a comparison between 3 iron lines in the spectra of the Sun and those of HER 165 and HER 240, predicted to be close to solar temperature on the basis of the photometric calibrations of, respectively, Soderblom et al. (1993) and Casagrande et al. (2006). Our spectroscopic analysis indicates, instead, a higher temperature. In the top panel of Fig. 1 the observed spectra are plotted, in the central panel we show synthetic models of the iron lines obtained by using, for HER 240 and HER 165, the parameters found in the spectroscopic analysis, and in the bottom panel we show the same spectral synthesis but with photometric temperature instead of the adopted one. The synthetic profiles based on spectroscopic temperatures resemble much more closely the observed ones. In particular, we note that, assuming a photometric temperature for HER 240, its spectrum is expected to match almost exactly that of the Sun, which is not the case. The region indicated was chosen to contain several Fe I lines in a narrow range.

The results of the chemical analysis are summarised in Table 4. Errors in the [X/H] values are those computed considering the uncertainty in the parameters and in the EWs, while the σ columns indicate the standard deviation of the measurements from individual lines. When only 2 or 3 lines are present, the standard deviation is replaced by half of the difference between the largest and the smallest value. Iron abundances in giant stars and relative errors are from Santos et al. (2009).

3.1. Oxygen abundances

To determine oxygen abundances, the only line available to us is the forbidden O I line at 6300.30 Å, which is very weak

		T$_{eff}$			logG	
Star	S08	HM	R06	S08	HM	R06
IC 4756 No38	5225±26	5151±73	5226	3.16±0.22	3.16±0.17	3.09
IC 4756 No42	5240±26	5217±89	5231	3.14±0.22	3.21±0.17	3.18
IC 4756 No125	5207±26	5146±82	5257	3.06±0.26	3.11±0.18	3.13
NGC 5822 No102	5253±28	5170±42	5260	3.17±0.39	3.20±0.13	3.28
NGC 5822 No224	5214±28	5237±65	5277	3.14±0.20	3.37±0.12	3.29
NGC 5822 No438	5208±25	5148±62	5208	3.16±0.19	3.21±0.11	3.19
		ξ			[Fe/H]	
	S08	HM	R06	S08	HM	R06
IC 4756 No38	1.40±0.02	1.22±0.11	1.35	0.05±0.08	0.08±0.11	0.09
IC 4756 No42	1.39±0.02	1.15±0.13	1.26	0.01±0.08	0.10±0.11	0.12
IC 4756 No125	1.47±0.02	1.31±0.13	1.23	0.02±0.08	0.07±0.11	0.10
NGC 5822 No102	1.44±0.03	1.18±0.07	1.28	0.00±0.08	0.05±0.06	0.04
NGC 5822 No224	1.41±0.03	1.15±0.08	1.29	0.06±0.08	0.22±0.08	0.21
NGC 5822 No438	1.39±0.02	1.13±0.08	1.19	0.06±0.08	0.18±0.08	0.14

Table 1. Comparison of abundance and parameter measurements for giants.

Star	V	B-V	T$_{Soder.}$	T$_{Casag.}$	T$_{spec}$	log G	ξ
						[log($g\ cm\ sec^2$)]	
	mag		[K]				[km·sec^{-1}]
IC 4756							
HER 97	13.38	0.85	5512	5418	6118	4.46	1.29
HER 165	13.50	0.81	5658	5562	6070	4.45	1.24
HER 240	13.48	0.76	5848	5753	6007	4.54	1.21
NGC 5822							
TATM 11003	14.662	0.769	5625	5546	6160	4.74	1.05
TATM 11014	14.448	0.732	5764	5685	6273	4.74	1.26

Table 3. Stellar parameters.

and often contaminated by telluric lines. We analysed this line using MOOG (Sneden 1973, version 2002) and Kurucz models (Kurucz 1993). The line is blended with that of Ni I at 6300.336 Å. As in Randich et al. (2006) and Pace et al. (2008), we assumed a log gf value of -2.11 for the oxygen line and and -9.717 for that of the nickel. To measure abundances in dwarfs, we selected the spectra for which the telluric lines did not overlap with the oxygen profile. Even after summing these spectra, the S/N ratio at the wavelength of interest remained too low to reliably measure the EW of the the blended feature or to compare the spectra with a synthetic model. We could only set an upper limit. Comparing the stellar feature with that of the UVES–archive solar spectrum, we noted that, in all the cases, the solar feature was well suited as an upper limit to the stellar one. We employed the driver $synthe$ of MOOG, assuming as fixed input the stellar parameters and nickel abundances obtained as described above, to compile the models of our stars; we then searched for the oxygen abundances for which the synthetic spectrum matched the solar one most closely, thus finding an upper limit to the stellar oxygen abundance. For the Sun itself, the match between synthetic and observed profile was achieved by assuming that log (O/H)+12=8.83±0.03. This value was subtracted from all the stellar values previously obtained, to determine

an upper limit to [O/H]. For all the 3 stars in IC 4756, we claim that [O/H] ≤ 0.15 dex. For the spectrum of HER 165, which is similar to that of the Sun, we estimate that the oxygen abundance of this star is not much lower than the aforementioned upper limit, but, owing to the scantiness of the data on which it depends, this conclusion must be interpreted with caution. For NGC 5822 dwarfs, we could find only an upper limit of 0.3 dex.

Despite the spectra for giants at our disposal being of high quality, we could not obtain precise measurements because the oxygen line was blended with the telluric feature at 6299 Å, and no calibration target was available to us. The centre of the telluric line coincided exactly with that of the oxygen line in the IC 4756 spectra, producing a single Gaussian feature. In the NGC 5822 spectra, the two line centers were separated sufficiently to create a slightly asymmetric feature, but in no case was it possible to achieve reliable results by the comparing the observed spectra with the synthetic ones. However, the telluric line at 6302 Å was isolated, and its EW ranged from 15 to 25 mÅ in all the spectra. The telluric line at 6299 Å, which is blended with the oxygen line, is a few percent stronger. We thus inferred that oxygen abundances in giants of both IC 4756 and NGC 5822 must be between -0.1 and 0.15 dex. Unfortunately, the direct comparison of giants and dwarfs

Star or Cluster name	Fe I			Na I			Al I			Si I		
	[X/H]	N	σ	[X/H]	N	σ	[X/H]	N	σ	[X/H]	N	σ
						dwarfs						
HER 165	0.05± 0.09	62	0.04	-0.10± 0.06	3	0.03	-0.01± 0.05	1	0.00	0.01± 0.02	8	0.04
HER 240	-0.02± 0.09	62	0.05	-0.17± 0.06	3	0.06	-0.20± 0.05	2	0.04	-0.06± 0.02	8	0.03
HER 97	0.00± 0.09	61	0.06	-0.18± 0.06	3	0.08	-0.06± 0.05	1	0.00	-0.07± 0.03	8	0.03
						mean dwarf						
IC 4756	0.01			-0.15			-0.09			-0.04		
						giants						
No 38	0.08± 0.11	16	0.08	0.19±0.04	3	0.04	-0.04±0.03	2	0.03	0.10±0.02	9	0.06
No 42	0.10± 0.11	15	0.08	0.23±0.03	3	0.05	-0.03±0.03	2	0.05	0.11±0.02	9	0.06
No 125	0.07± 0.11	15	0.08	0.16±0.04	3	0.04	-0.03±0.03	2	0.04	0.09±0.02	9	0.05
						mean giant						
IC 4756	0.08			0.19			-0.03			0.10		
						dwarfs						
TATM 11014	0.07± 0.09	49	0.05	-0.11± 0.06	3	0.05	-0.05± 0.05	1	0.00	0.04± 0.03	6	0.03
TATM 11003	0.02± 0.09	57	0.07	-0.19± 0.06	2	0.03	–	–	–	-0.01± 0.03	7	0.05
						mean dwarf						
NGC 5822	0.05			-0.15			-0.05			0.01		
						giants						
No 102	0.05± 0.06	13	0.04	0.15±0.03	3	0.09	-0.04±0.02	2	0.09	0.03±0.02	9	0.09
No 224	0.22± 0.08	14	0.06	0.26±0.03	3	0.05	0.05±0.02	2	0.06	0.18±0.02	9	0.07
No 438	0.18± 0.08	16	0.06	0.23±0.03	3	0.05	0.05±0.02	2	0.05	0.20±0.02	9	0.12
						mean giant						
NGC 5822	0.15			0.21			0.02			0.14		

Star or Cluster name	Ca I			Ti I			Cr I			Ni I		
						dwarfs						
HER 165	0.10± 0.08	9	0.04	0.02± 0.10	11	0.06	0.05± 0.11	6	0.05	-0.03± 0.06	21	0.05
HER 240	-0.01± 0.08	11	0.03	-0.05± 0.10	10	0.06	0.00± 0.11	6	0.05	-0.09± 0.06	22	0.05
HER 97	0.06± 0.08	11	0.06	-0.08± 0.10	11	0.12	-0.04± 0.11	5	0.04	-0.07± 0.07	20	0.07
						mean dwarf						
IC 4756	0.05			-0.04			0.00			-0.06		
						giants						
No 38	0.06±0.05	9	0.04	0.11±0.07	9	0.08	0.08±0.07	6	0.03	0.03±0.03	23	0.07
No 42	0.09±0.05	9	0.05	0.15±0.07	9	0.09	0.14±0.07	6	0.03	0.05±0.03	23	0.07
No 125	0.03±0.05	9	0.05	0.08±0.07	9	0.08	0.05±0.07	6	0.04	0.05±0.03	23	0.08
						mean giant						
IC 4756	0.06			0.11			0.08			0.04		
						dwarfs						
TATM 11014	0.09± 0.08	9	0.05	0.01± 0.09	6	0.07	0.11± 0.10	6	0.04	-0.01± 0.06	21	0.06
TATM 11003	0.06± 0.08	9	0.04	-0.02± 0.10	9	0.04	0.04± 0.11	6	0.10	-0.06± 0.06	19	0.07
						mean dwarf						
NGC 5822	0.08			0.00			0.07			-0.03		
						giants						
No 102	0.02±0.03	9	0.06	0.07±0.05	9	0.08	0.09±0.05	6	0.05	-0.11±0.02	23	0.09
No 224	0.16±0.03	9	0.07	0.28±0.05	9	0.08	0.24±0.05	6	0.03	0.17±0.02	23	0.10
No 438	0.14±0.03	9	0.05	0.19±0.05	9	0.09	0.21±0.05	6	0.03	0.14±0.02	23	0.09
						mean giant						
NGC 5822	0.11			0.18			0.18			0.07		

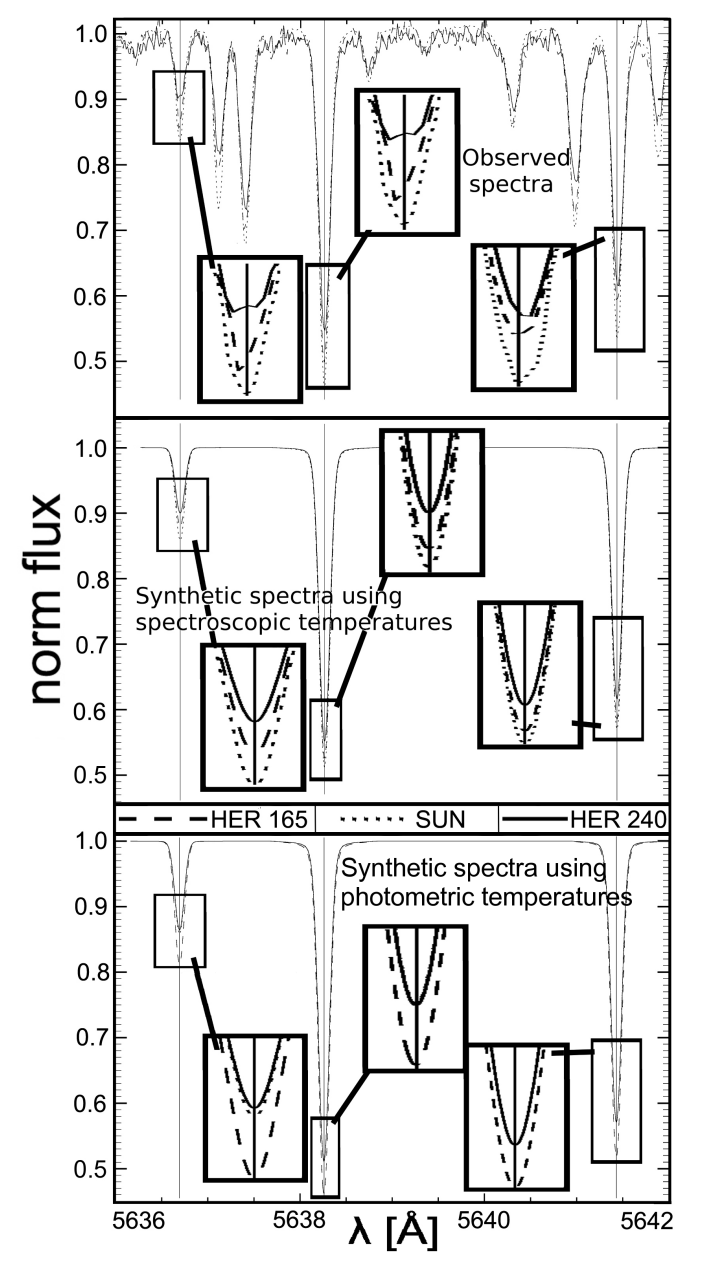**Table 4.** Results of the chemical analysis.

Fig. 1. Comparison of the spectra of HER 240 and HER 165 with that of the Sun.

in the same cluster on the basis of these approximations, does not add relevant information.

3.2. Lithium

Lithium abundances were obtained by analysing the lithium doublet at 6707.8 Å. Adopting a procedure similar to that used for oxygen, we employed the driver *synthe* of MOOG, the line list from Israelian et al. (2001), and Kurucz models obtained with the stellar parameters measured above, to produce synthetic spectra in the wavelength interval encompassing the lithium line profile, and searched for the lithium abundance for which the closest match to the observed feature is achieved. We were able to obtain reliable measurements because the profiles are quite strong

in our stars. The typical errors, across the lithium abundance range for which the match was acceptable, are between 0.05 and 0.15 dex. If we were to adopt the conservative estimate of 110 K for the error in the temperature as in Pace et al. (2008), this would lead to an uncertainty in the lithium abundance of 0.1 dex, which would imply a typical maximum error of about 0.15 dex. The other parameters hardly affect the lithium abundance determination. Using the same procedure, we also compared the synthetic spectrum of the Sun with the UVES–archive solar spectrum, finding that we obtained the closest match by assuming A(Li)= 1 rather than the canonical A(Li)=1.1 where A(Li) is, as is customary, $\log(\mathrm{Li/H})+12$.

Since we believe that a more precise temperature scale may improve our understanding of lithium depletion (Sect. 3.2) and errors in the colour excess may introduce a cluster to cluster bias in the temperature determinations (cf. Sect. 3), we measured the lithium abundances of stars in the sample of Pace et al. (2008) for which data in the literature were based on photometric temperatures, and whose parent clusters are significantly reddened and photometric temperatures, as a consequence, were uncertain. The results of our lithium abundance measurements are shown in Table 3.2, in dex, along with temperature, in Kelvin, and gravity, in unit of $\log~(\mathrm{g \cdot cm \cdot sec^{-2}})$. Since, using the same method, the Sun is found to have A(Li)=1.0, the data are probably more comparable to literature sources when a positive offset of 0.1 dex is added.

In Fig. 2, we also show a temperature versus lithium abundance diagram, in which we compare the 12 data points from the present analysis, shown in Table 3.2, with published open cluster data at 3 different ages. Data for M 67 are taken from Pasquini et al. (2008), the remainder being from the compilation in Xiong & Deng (2009). For clarity, literature data were represented with curves instead of datapoints, drawn by eye in the region around which the datapoints would cluster. Hyades, Coma, and Praesepe data are depicted in a single curve, another represents NGC 752, and a third M 67. The ages indicated are taken from Salaris et al. (2004). The temperatures for the Hyades age clusters and NGC 752 are derived from photometry. For the former, the uncertainty in the colour excess should not play a major role, since they are nearby clusters.

The additional 12 points introduced in Fig. 2 clearly do not account for all unsolved problems in mixing and lithium depletion in solar–type stars. Nevertheless, the steeper decline of lithium abundance in IC 4651 suggests that a study of a larger sample of stars in this cluster would be warranted.

4. Rotation velocity

In Pace & Pasquini (2004) we obtained, using available UVES spectra, the cross–correlation profile with a suitable template (courtesy of C. Melo) and measured its FWHM for a set of stars with published $v \cdot \sin i$ taken with the same configuration as for those of the targets; we found the values of A and B that minimise the χ^2 in the relationship

$$v \cdot \sin i = A \cdot \sqrt{FWHM^2 - B^2}.$$

We then used that relationship with the computed values of A and B, to measure target–star $v \cdot \sin i$ from the FWHM of their cross–correlation profile. For the present analysis

Star	A(Li)	T_{eff}	logG
Present sample			
IC 4756 ([Fe/H]=0.01 dex)			
HER 97	2.75	6118	4.46
HER 165	2.8	6070	4.45
HER 240	2.6	6007	4.54
NGC 5822 ([Fe/H]=0.05 dex)			
TATM 11003	2.8	6160	4.74
TATM 11014	2.5	6273	4.74
Sample of Pace et al. (2008)			
IC 4651 ([Fe/H]=0.12 dex)			
AHTC 1109	2.7	6060	4.55
AHTC 2207	2.5	6050	4.36
AHTC 4220	2.1	5910	4.57
AHTC 4226	2.1	5980	4.44
Eggen 45	2.7	6320	4.43
NGC 3680 ([Fe/H]=-0.04 dex)			
Eggen 70	2.8	6210	4.47
AMC 1009	2.5	6010	4.50

Table 5. Lithium abundance measurements.
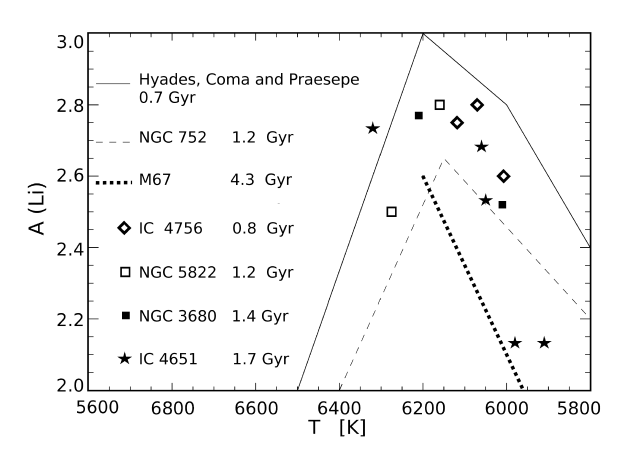
Fig. 2. Comparison of lithium abundances in different open clusters.

we repeated the calibration with the same stars, obtaining the cross–correlation profiles of calibration and target stars with the IRAF command $f$xcor using the upper red arm of UVES spectra (from 5800 to 6800 Å) and, as a template, the UVES archive solar spectrum. This new calibration made our measurements easier to reproduce. Calibration data – namely star names, FWHM, $v \sin i$, and deviations from the fit – are shown in Table 6. We found the following values for the parameters in the equation above: $A = 0.82$ [km·sec^{-1}], $B = 5.93$ pixels, giving a root mean square of the data points around the fit of 1.5 km·sec^{-1}. We adopt this value

Star	FWHM [pixels]	$v \sin i$ [km·sec^{-1}]	dev. [km·sec^{-1}]
Sun	5.46	2.0	-2.0
stars in IC 4651:			
AT 1228	17.74	15.7	-1.9
Eggen 15	11.76	10.0	-1.6
Eggen 34	32.19	25.2	0.9
Eggen 45	7.56	4.2	-0.3
Eggen 79	25.6	21.8	-1.3
Eggen 99	36.28	28.1	1.4
star in NGC 3680:			
Eggen 60	7.10	1.9	1.3

Table 6. Data used to calibrate the $v \sin i$.

Star	FWHM [pixels]	$v \sin i$ [km·sec^{-1}]
IC 4756		
HER 165	6.9	3
HER 97	8.1	5
HER 240	7.0	3
NGC 5822		
TATM 11014	8.9	5
TATM 11003	7.1	3

Table 7. $v \sin i$ estimations of our target stars.

as an estimate of the uncertainty in the $v \sin i$ measurement due to the calibration Δ_{cal}

The results for projected rotation velocities are given in Table 7. We also computed the error in FWHM from the standard deviation of the FWHM measurements performed on the individual spectra, and when only two spectra were available for a given star, half of the difference between the two measurements were used. The error in FWHM measurement was found to be much smaller than Δ_{cal}. However, the results provide only a rough estimate. The stars of our sample appear to rotate slightly more rapidly than the Sun, for which $v \sin i$=2 km·sec^{-1}, and similarly to the solar stars in IC 4651 and NGC 3680. These slow rotators in young clusters are not surprising, since Pace & Pasquini (2004) measured low values of $v \sin i$ also in Hyades and Praesepe stars. The data presented in Table 7 alone, is not sufficient to allow us to draw conclusions about the evolution of angular momentum in solar type stars.

5. Comparison of our chemical abundances with previous results

In Table 8, we compiled abundance measurements available in the literature, by means of spectroscopic studies. We indicated the dispersion in the measurements, using either their standard deviation or, when only 3 or 2 measurements were available, half of the difference between the highest and lowest value. The measurements given by Gilroy (1989)

Cluster	source	[Fe/H]	[Na/H]	[Al/H]	[Si/H]	Ref
IC 4756	3 dwarfs	0.01 σ=0.04	-0.15 σ= 0.04	-0.09 σ=0.05	-0.04 σ=0.04	1
IC 4756	1 dwarf	0.03 –				4
IC 4756	3 giants	0.08 σ=0.02	0.19 σ= 0.04	-0.03 σ=0.05	0.10 σ=0.01	1,2
IC 4756	7 giants	0.0 ±0.1 *				3
IC 4756	4 giants	-0.05 ±0.04				4
IC 4756	1 giant			0.20	0.16±0.25	4
IC 4756	6 giants	-0.15 σ=0.04	0.73 σ= 0.06 *	0.44 σ=0.08 *	0.19 σ=0.06	5
NGC 5822	2 dwarfs	0.05 σ=0.03	-0.15 σ= 0.04	-0.05 –	0.01 σ=0.02	1
NGC 5822	3 giants	0.15 σ=0.08	0.21 σ= 0.04	0.02 σ=0.01	0.14 σ=0.08	1,2
NGC 5822	3 giants	0.12 σ=0.1				4
NGC 5822	1 giant		0.28±0.07	0.12±0.12	0.25±0.25	4
		[Ca/H]	[Ti/H]	[Cr/H]	[Ni/H]	
IC 4756	3 dwarfs	0.05 σ=0.05	-0.04 σ= 0.05	0.00 σ=0.05	-0.06 σ=0.03	1
IC 4756	3 giants	0.06 σ=0.03	0.11 σ= 0.03	0.08 σ=0.03	0.04 σ=0.01	1,2
IC 4756	1 giant	-0.06±0.29	-0.28±0.29		0.04±0.16	4
IC 4756	6 giants	-0.08 σ=0.08			-0.07 σ=0.05	5
NGC 5822	2 dwarfs	0.08 σ=0.02	0.00 σ= 0.02	0.07 σ=0.04	-0.03 σ=0.03	1
NGC 5822	3 giants	0.11 σ=0.07	0.18 σ= 0.11	0.18 σ=0.08	0.07 σ=0.14	1,2
NGC 5822	1 giant	-0.05±0.23	0.20±0.24	0.26±0.29	0.25±0.26	4

Table 8. Compilation of abundance determinations in the literature from spectroscopic data. References: (1) Present work; (2) Santos et al. (2009); (3) Gilroy (1989); (4) Luck (1994); (5) Jacobson et al. (2007)

(flagged with an asterisk) have only two significant digits, and for 5 out of 7 stars resulted to have [Fe/H]=0.0 dex. The value indicated in this table is more representative of her results than the mean of the 7 measurements (which would be 0.04 dex). The measurements by Jacobson et al. (2007) marked with an asterisk refer to the EW analysis result. Spectral synthesis indicate an enhancement 0.06 dex higher for sodium and 0.11 dex lower for aluminium.

We note that the iron abundance measurement of giants in IC 4756 made by Jacobson et al. (2007) are substantially lower than any other quoted result, including that of the present analysis and of Santos et al. (2009). Jacobson et al. employed Hydra/WIYN spectra at a resolution of R≈15 000, whose S/N range from 75 to 150 per pixel, and whose spectral coverage is 300 Å, enough to include more than 20 Fe ɪ lines and 3 or 4 Fe ɪɪ lines. Furthermore, they analysed 6 giants, and their measurements show little spread. Sousa et al. (2007) showed that, for a spectrum of a dwarf with S/N of about 100 per pixel, at resolutions lower than R≈30 000, EWs are systematically underestimated. For R=15 000, this effect is about 10%, leading to abundance errors that might account for the mismatch between our results and those of Jacobson. Giants are likely to be more strongly affected, because of their higher line crowding. However, for abundance ratios [X/Fe], these effects, which affect both sides of the ratio, should compensate each other.

Data shown in Table 8 indicate that there is a difference in the chemical composition between giants and dwarfs. In particular, sodium abundance is significantly enhanced in giants. The huge discrepancy between different enhancements found, e.g., in the present work and Jacobson et al. (2007), is mainly due to the use of a different line list. These authors claim that were they to use the same line list we employed (Randich et al. 2006), they would find [Na/H]=0.2, which matches our result for giants.

6. Revision of cluster fundamental parameters

The new iron abundance estimates that we provide in this paper offer us the possibility of revising the cluster fundamental parameters - namely distance, reddening and age - on a more solid basis. Therefore, we collated the available photometry from the literature, and created colour magnitude diagrams (CMD). We adopted Herzog et al. (1975) photographic photometry for IC 4756 and Twarog et al. (1993) CCD photometry for NGC 5822. The two CMDs are shown in the right and left panel of Fig. 3, respectively. We transformed iron abundances values from the logarithmic scale relative to the Sun ([Fe/H]) into the linear scale (Z) using the relation [Fe/H] = log (Z/0.019) from Carraro et al. (1999). We then generated isochrones for that value of Z. We obtained Z = 0.019 for IC 4756 and Z = 0.021 for NGC 5822. In Fig. 3, we show the best fit *by eye* that we achieved after several trials. The fit to the CMD of NGC 5822 (left panel) is good providing the set of parameters: E(B-V) = 0.1± 0.05, (m-M) = 9.9±0.1, and age = 1.0±0.1 Gyr. This, in turn, yields a heliocentric distance of 830 pc. The CMD of IC 4765 has a much larger spread and a secondary main sequence (MS), presumably produced by binary stars, and
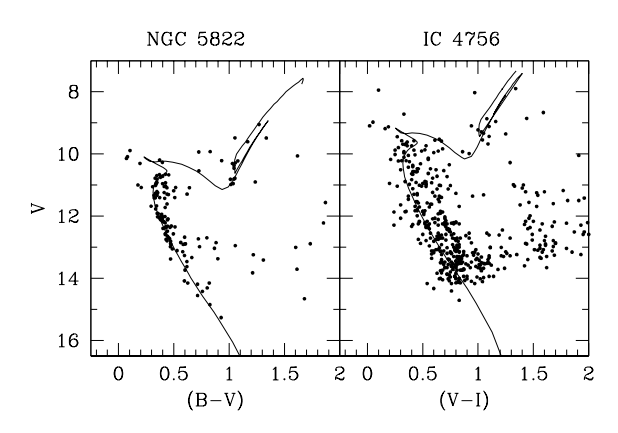
Fig. 3. CMD and fit of isochrones for NGC 5822 and IC 4756.

which seems to be as populated as the single star MS. For this cluster, our parameters are E(B-V) = 0.15±0.10, (m-M) = 8.6±0.1, and age = 0.8±0.2 Gyr. This, in turn, yields a heliocentric distance of 430 pc.

As noted in Sect. 3, the huge differences between photometric and spectroscopic temperatures imply that a zero–point error exist in the photometry of roughly 0.13 mag for NGC 5822, and of the same order of magnitude for IC 4756 but more difficult to evaluate due to the differential reddening. This can explain the difference between the extinctions obtained in this section and those obtained in the extinction maps of Hakkila et al. (1997) as described in Meléndez et al. (2006). The aforementioned zero–point error affects the present evaluation of the cluster parameters by an amount that should be added to random errors (the errors given above include it). The age evaluation, however, is not significantly affected by this.

In both cases, we highlight the need for improved photometry to reach fainter magnitudes along the MS, and comparison fields to deal with contamination. These are of primary importance for at least two reasons. More precise age estimates will firstly allow us to either confirm or revise the conclusions reached in Pace et al. (2009) concerning the evolution of chromospheric activity. Secondly, we will be able to say whether the cause of the discrepancy between photometric and spectroscopic temperatures resides completely in the photometry, as we suspect, or whether a systematic error in our spectroscopic temperature determinations is present and should be corrected for.

7. Conclusions.

We have analysed high resolution spectra of 5 solar–type stars in IC 4756 and NGC 5822 to obtain their parameters, chemical composition, including lithium abundances, and estimates of their projected rotation velocities. While our iron abundances, in most cases, are consistent within the errors, with those of previous studies for giants of the same

clusters, sodium, aluminium and silicon, present very high enhancements in giants in IC 4756. This finding agrees with published results of several other open clusters (see Sect. 1). Regardless of whether these abundance enhancements are real or due to systematic errors, they have important implications (De Silva et al. 2009); for example in the studies of chemical evolution of the Galactic bulge, when comparing the bulge with the disk, the same type of stars in both populations should be used. In the first studies of this kind employing high–resolution spectroscopy, this was not yet possible for a sufficient number of targets (Fulbright et al. 2007; Lecureur et al. 2007; Zoccali et al. 2006). But works are presently available that compare bulge giants with disk giants (e.g., Meléndez et al. 2008; Alves–Brito et al. 2010; Ryde et al. 2010) or bulge dwarfs with disk dwarfs, taking advantage of the microlensing effect (e.g., Bensby et al. 2009). The rotation velocity of our sample stars is slightly larger than that of the Sun, roughly between 3 and 5 km·sec^{-1}, a smaller range than observed in other clusters of comparable age.

Cluster parameters are computed using published photometry and the iron abundance obtained in the spectroscopic analysis. We found an age of 1 Gyr for NGC 5822 and 0.8 Gyr for IC 4756. However, for IC 4756 in particular, new photometry would considerably reduce the uncertainties. This is of crucial importance owing to the impact of the ages of these clusters on the characterisation of the evolution of chromospheric activity.

We compared lithium abundances with published cluster data at 3 different ages, and with measurements made on stars in intermediate age clusters from our sample of Pace et al. (2008). Most of the stars studied by us have lithium abundance levels lying between that of NGC 752 and that of the Hyades–age clusters. Even though based on only 4 datapoints, we see evidence that a steep decline in lithium abundances occurs below 6 000 K in IC 4651.

Accurate determinations of temperature and lithium abundances in more member stars of such clusters as IC 4651 would clearly be invaluable in understanding the reason for differences among clusters.

References

Alves-Brito, A., Meléndez, J., Asplund, M., Ramírez, I.,& Yong, D. 2010, A&A, accepted
Bensby, T., et al. 2009, arXiv:0911.5076, A&A, accepted
Bragaglia, A., & Tosi, M. 2006, AJ, 131, 1544
Carraro, G., Ng, Y. K., & Portinari, L. 1998, MNRAS, 296, 1045
Carraro, G., Girardi, L., & Chiosi, C. 1999, MNRAS, 309, 430
Carraro, G., Bresolin, F., Villanova, S., Matteucci, F., Patat, F., & Romaniello, M. 2004, AJ, 128, 1676
Carraro, G., Geisler, D., Villanova, S., Frinchaboy, P. M., & Majewski, S. R. 2007, A&A, 476, 217

Casagrande, L., Portinari, L., & Flynn, C. 2006, MNRAS, 373, 13

De Silva, G. M., Gibson, B. K., Lattanzio, J., & Asplund, M. 2009, arXiv:0905.4354

Dias, W. S., & Lépine, J. R. D. 2005, ApJ, 629, 825

D'Orazi, V., & Randich, S. 2009, arXiv:0905.1835

Edvardsson, B., Andersen, J., Gustafsson, B., Lambert, D. L., Nissen, P. E., & Tomkin, J. 1993, A&A, 275, 101

Friel, E. D., Janes, K. A., Tavarez, M., Scott, J., Katsanis, R., Lotz, J., Hong, L., & Miller, N. 2002, AJ, 124, 2693

Friel, E. D., Jacobson, H. R., Barrett, E., Fullton, L., Balachandran, S. C., & Pilachowski, C. A. 2003, AJ, 126, 2372

Friel, E. D., Jacobson, H. R., & Pilachowski, C. A. 2005, AJ, 129, 2725

Fulbright, J. P., McWilliam, A., & Rich, R. M. 2007, ApJ, 661, 1152

Gilroy, K. K. 1989, ApJ, 347, 835

Hakkila, J., Myers, J. M., Stidham, B. J., & Hartmann, D. H. 1997, AJ, 114, 2043

Hekker, S., & Meléndez, J. 2007, A&A, 475, 1003

Israelian, G., Santos, N. C., Mayor, M., & Rebolo, R. 2001, Nature, 411, 163

Jacobson, H. R., Friel, E. D., & Pilachowski, C. A. 2007, AJ, 134, 1216

Jacobson, H. R., Friel, E. D., & Pilachowski, C. A. 2009, AJ, 137, 4753

Herzog, A. D., Sanders, W. L., & Seggewiss, W. 1975, A&AS, 19, 211

Lecureur, A., Hill, V., Zoccali, M., Barbuy, B., Gómez, A., Minniti, D., Ortolani, S., & Renzini, A. 2007, A&A, 465, 799

Luck, R. E. 1994, ApJS, 91, 309

Kurucz, R.L. 1993, ATLAS9 Stellar Atmosphere Programs (Kurucz CD-ROM No. 13)

Magrini, L., Sestito, P., Randich, S., & Galli, D. 2009, A&A, 494, 95

Mashonkina, L. I., Shimanskiĭ, V. V., & Sakhibullin, N. A. 2000, Astronomy Reports, 44, 790

Meléndez, J., Shchukina, N. G., Vasiljeva, I. E., & Ramírez, I. 2006, ApJ, 642, 1082

Meléndez, J., et al. 2008, A&A, 484, L21

Mermilliod, J.-C., & Mayor, M. 1990, A&A, 237, 61

Mermilliod, J. C., Mayor, M., & Udry, S. 2008, A&A, 485, 303

Pace, G., & Pasquini, L. 2004, A&A, 426, 1021

Pace, G., Pasquini, L., & François, P. 2008, A&A, 489, 403

Pace, G., Melendez, J., Pasquini, L., Carraro, G., Danziger, J., François, P., Matteucci, F., & Santos, N. C. 2009, A&A, 499, L9

Pasquini, L., Randich, S., Zoccali, M., Hill, V., Charbonnel, C., & Nordström, B. 2004, A&A, 424, 951

Pasquini, L., Biazzo, K., Bonifacio, P., Randich, S., & Bedin, L. R. 2008, A&A, 489, 677

Paulson, D. B., Sneden, C., & Cochran, W. D. 2003, AJ, 125, 3185

Randich, S., Sestito,P., Primas, F., Pallavicini, R., & Pasquini, L. 2006, A&A, 450, 557

Ryde, N., et al. 2010, A&A, 509, A260000

Salaris, M., Weiss, A., & Percival, S. M. 2004, A&A, 414, 163

Santos, N. C., Lovis, C., Pace, G., Melendez, J., & Naef, D. 2009, A&A, 493, 309

Schmidt, E. G. 1978, PASP, 90, 157

Sestito, P., Randich, S., & Bragaglia, A. 2007, A&A, 465, 185

Smiljanic, R., Pasquini, L., Charbonnel, C., & Lagarde, N. 2009, arXiv:0910.4399

Sneden, C. 1973, ApJ, 184, 839

Soderblom, D. R., Stauffer, J. R., Hudon, J. D., & Jones, B. F. 1993, ApJS, 85, 315

Sousa, S. G., Santos, N. C., Israelian, G., Mayor, M., & Monteiro, M. J. P. F. G. 2007, A&A, 469, 783

Sousa, S. G., et al. 2008, A&A, 487, 373

Tautvaišiene, G., Edvardsson, B., Tuominen, I., & Ilyin, I. 2000, A&A, 360, 499

Tautvaišienė, G., Edvardsson, B., Puzeras, E., & Ilyin, I. 2005, A&A, 431, 933

Twarog, B. A., Anthony-Twarog, B. J., & McClure, R. D. 1993, PASP, 105, 78

Villanova, S., Carraro, G., & Saviane, I. 2009, arXiv:0906.4330

Xiong, D. R., & Deng, L. 2009, MNRAS, 395, 2013

Zoccali, M., et al. 2006, A&A, 457, L1